Semiclassical echo dynamics in the Sachdev-Ye-Kitaev model

Markus Schmitt,[1,2,3,*] Dries Sels,[4,5,6] Stefan Kehrein,[1] and Anatoli Polkovnikov[4]

[1]*Institute for Theoretical Physics, Georg-August-Universität Göttingen, Friedrich-Hund-Platz 1, 37077 Göttingen, Germany*
[2]*Max Planck Institute for the Physics of Complex Systems, Nöthnitzer Straße 38, 01187 Dresden, Germany*
[3]*Department of Physics, University of California, Berkeley, California 94720, USA*
[4]*Department of Physics, Boston University, 590 Commonwealth Avenue, Boston, Massachusetts 02215, USA*
[5]*Department of Physics, Harvard University, 17 Oxford Street, Cambridge, Massachusetts 02138, USA*
[6]*Theory of Quantum and Complex System, Universiteit Antwerpen, Universiteitsplein 1, B-2610 Antwerpen, Belgium*

The existence of a quantum butterfly effect in the form of exponential sensitivity to small perturbations has been under debate for a long time. Lately, this question has gained increased interest due to the proposal to probe chaotic dynamics and scrambling using out-of-time-order correlators. In this work we study echo dynamics in the Sachdev-Ye-Kitaev model under effective time reversal in a semiclassical approach using the truncated Wigner approximation, which accounts for nonvanishing quantum fluctuations that are essential for the dynamics. We demonstrate that small imperfections introduced in the time-reversal procedure result in an exponential divergence from the perfect echo, which allows us to identify a Lyapunov exponent λ_L. In particular, we find that λ_L is twice the Lyapunov exponent of the semiclassical equations of motion. This behavior is attributed to the growth of an out-of-time-order double commutator that resembles an out-of-time-order correlator.

I. INTRODUCTION

The question of chaos and the possibility of a butterfly effect in quantum systems are a long-standing problem that has received increased attention in recent years. In studies addressing the information paradox of black holes, so-called out-of-time-order correlators (OTOCs) of the form

$$\langle \hat{V}(0)^\dagger \hat{W}(t)^\dagger \hat{V}(0)\hat{W}(t)\rangle_\beta \tag{1}$$

were introduced to probe the sensitivity of the dynamics to small perturbations and scrambling, i.e., the delocalization of initially local information [1–4]. A semiclassical analysis of the OTOC motivates that it can exhibit exponential growth, allowing the identification of a Lyapunov exponent [5]. In fact, it was found that in a black-hole theory OTOCs grow exponentially with the maximal possible rate $\lambda_L = \frac{2\pi}{\beta}$ [6]. Remarkably, there exists a solvable model of interacting fermions, which also saturates this bound at low temperatures, namely, the Sachdev-Ye-Kitaev (SYK) model [7,8], which is a variant of a model originally introduced by Sachdev and Ye [9,10].

OTOCs as a dynamical probe of chaos and scrambling are also of interest in condensed-matter systems beyond the anti-de Sitter/conformal field theory (AdS/CFT) paradigm [11–18]. Particularly intriguing is the connection to the question of how and in what sense closed quantum many-body systems thermalize when initially prepared far from equilibrium, which has been studied with great efforts in recent years [19,20]. The corresponding statistical description of the stationary state is justified only if the

information about the initial state cannot be recovered in practice; that is, the dynamics is irreversible.

To assess the irreversibility of the dynamics a common approach is to study imperfect effective time reversal. In classical systems it is understood that the exponential sensitivity of the dynamics to small perturbations prohibits recovery of the initial state because perfect time reversal is impossible in practice [21–24]. Under chaotic dynamics any imperfection occurring in the time-reversal operation leads to an exponential divergence from accurate recovery of the initial state with a rate that is largely independent of the perturbation, namely, the Lyapunov exponent. This renders the improvement of the protocol prohibitively expensive.

Analogous approaches have been explored considering quantum systems. In few-body systems the decay characteristics of the Loschmidt echo $\mathcal{L}(\tau) = |\langle\psi_0|\hat{U}_E^\epsilon(\tau)|\psi_0\rangle|^2$ with the echo operator $\hat{U}_E^\epsilon(\tau) = e^{i(\hat{H}+\epsilon\hat{V})\tau}e^{-i\hat{H}\tau}$, where $\epsilon\hat{V}$ constitutes a small perturbation to the Hamiltonian, were used as an indicator of chaos and irreversibility [25–27]. For many-body systems, however, overlaps lack experimental significance. Instead, the decay of observable echoes under imperfect effective time reversal was studied to investigate irreversibility [28–32].

In the works mentioned above the focus was on decay laws occurring in the echo dynamics at late times. By contrast, imperfect effective time reversal in classical systems features an initial dynamics that is governed by the butterfly effect. The possibility of a butterfly effect that occurs analogously in quantum systems is currently under debate [11,17,28,33–37]. Moreover, the realization of effective time reversal was recently reported from an experiment with trapped ions, where OTOCs were measured in the form of echo dynamics [38].

*markus.schmitt@berkeley.edu

In this work we study the dynamics of the SYK model under imperfect effective time reversal in a semiclassical approach using the truncated Wigner approximation. We demonstrate that the small imperfection leads to an exponential divergence from the perfect echo. This divergence can be attributed to the exponential growth of an out-of-time-order double commutator similar to an OTOC and it allows us to identify a Lyapunov exponent based on the echo dynamics.

The structure of the paper is as follows: First, in Secs. II and III we introduce the echo protocol under consideration and the model of interest. Section IV comprises an introduction to the truncated Wigner approximation and a discussion of its applicability to the SYK model. In Sec. V we present our results for the echo dynamics in the semiclassical limit. Before the final discussion in Sec. VII we include in Sec. VI an extended elaboration of the distinction between mean-field dynamics and the truncated Wigner approximation in the context of the SYK model.

II. IMPERFECT EFFECTIVE TIME REVERSAL

In the following we will investigate the echo dynamics of an observable $\hat{O}$ under imperfect effective time reversal. The perturbation is introduced by the action of a perturbation operator $\hat{P}_\epsilon$ on the time-evolved state at the point of time reversal. Here, ϵ denotes a parameter for the smallness of the perturbation. A natural choice for the perturbation operator is unitary time evolution for a short interval δt with a perturbation Hamiltonian $\hat{H}_p$, i.e., $\hat{P}_{\delta t} = e^{-i\hat{H}_p \delta t}$. The quantity of interest is the echo signal

$$E_{\hat{O}}(\tau) = \langle \psi_0 | \hat{U}_E^{\delta t}(\tau)^\dagger \hat{O} \hat{U}_E^{\delta t}(\tau) | \psi_0 \rangle, \quad (2)$$

with the echo operator $\hat{U}_E^{\delta t}(\tau) = e^{i\hat{H}\tau} \hat{P}_{\delta t} e^{-i\hat{H}\tau}$. This constitutes an OTOC in the case that the initial state is an eigenstate of the observable, $(\hat{O} - \mu)|\psi_0\rangle = 0$ [32,38]. Moreover, expanding the echo operator $\hat{U}_E^{\delta t}(\tau)$ in orders of δt yields

$$\Delta E_{\hat{O}}(\tau) = \langle \psi_0 | \hat{O} | \psi_0 \rangle - E_{\hat{O}}(\tau)$$
$$= i\delta t \langle \psi_0 | [\hat{H}_p(\tau), \hat{O}] | \psi_0 \rangle$$
$$+ \frac{\delta t^2}{2} \langle \psi_0 | [\hat{H}_p(\tau), [\hat{H}_p(\tau), \hat{O}]] | \psi_0 \rangle + O(\delta t^3) \quad (3)$$

for the divergence from the perfect echo. In this expression the linear term corresponds to the linear response, and it vanishes in the case in which the initial state is an eigenstate of the observable. Hence, the quadratic term constitutes the leading contribution to the divergence from the perfect echo, accounting for the sensitivity of the dynamics to small perturbations. Using the example of the SYK Hamiltonian, we will demonstrate in the following that this double commutator in fact determines the initial decay of the echo and that the corresponding divergence grows exponentially in time, which allows us to identify a Lyapunov exponent.

III. MODEL HAMILTONIAN

The Hamiltonian of the fermionic SYK model is given by

$$\hat{H} = \frac{1}{(2N)^{3/2}} \sum_{ijkl} J_{ij;kl} \hat{c}_i^\dagger \hat{c}_j^\dagger \hat{c}_k \hat{c}_l, \quad (4)$$

where $J_{ij;kl}$ are complex-valued Gaussian random couplings with vanishing mean and variance $\sigma^2 = \overline{|J_{ij;kl}|^2}$. N denotes the number of fermionic modes. The SYK model has a number of remarkable properties. Although strongly interacting, it is exactly solvable in the limit of large N. At low temperatures it exhibits an emergent conformal symmetry, indicating the existence of a holographic dual [8]. In this regime it is maximally chaotic in the sense that the Lyapunov exponent occurring in OTOCs saturates the bound that was derived for AdS black holes [6].

IV. SEMICLASSICAL DYNAMICS IN THE SYK MODEL

We will analyze echo dynamics using the fermionic version of the truncated Wigner approximation (TWA), which was recently developed in Refs. [39,40].

A. On the applicability of the truncated Wigner approximation

The TWA is the saddle point approximation for the Keldysh action describing the Heisenberg evolution of the observables. It can be generally derived using standard path integral methods [41]. Within the TWA time evolution of phase space variables is governed by the classical Hamiltonian equations of motion, which have to be supplemented by fluctuating initial conditions. In turn those are encoded in the Wigner function describing the initial state. Within the accuracy of the TWA one can generally approximate this Wigner function by a Gaussian capturing means and fluctuations of the phase space variables. Note that while, formally, classical equations of motion are identical to the Dirac mean-field equations of motion (see Sec. VI), the TWA reduces to the mean-field approximation only if fluctuations in initial conditions are asymptotically vanishing with the saddle point parameter. This is, e.g., the case for initial coherent states or for polarized quantum spins in the large-S limit. But it is not the case, e.g., for stationary states of a high-energy particle in a confining potential where the Wigner function approaches the broad in space microcanonical distribution rather than a single phase space point. In many instances, in particular when we deal with fermions or spin-1/2 degrees of freedom, fluctuations are always large, such that the mean-field approximation is generally incorrect and, moreover, is not approached as the saddle point parameter increases (see, e.g., Refs. [42,43]). In the SYK model the large-N limit ensures the validity of the saddle point approximation [8,44], and therefore, it is natural that the fermionic version of TWA will be asymptotically exact in the large-N limit, which, as we show in Sec. IV C, is indeed the case. Hence, N serves as an effective $\hbar^{-1}$.

B. Phase space approach for fermions

Within the fermionic TWA a phase space representation is constructed for the fermionic bilinears, which satisfy the commutation relations of $so(2N)$ [39,40]; see also Ref. [45] for a general picture of classical representations of quantum models. The Weyl symbols of the fermionic bilinears are $\tau_{\alpha\beta} = (\hat{c}_\alpha \hat{c}_\beta)_W = -(\hat{c}_\alpha^\dagger \hat{c}_\beta^\dagger)_W^*$ and $\rho_{\alpha\beta} = \frac{1}{2}(\hat{c}_\alpha^\dagger \hat{c}_\beta - \hat{c}_\beta \hat{c}_\alpha^\dagger)_W$. The corresponding Weyl symbol of the SYK Hamiltonian expressed

in terms of pairing operators is

$$\mathcal{H} = \frac{1}{(2N)^{3/2}} \sum_{ijkl} J_{ij;kl}(\tau_{ji}^* \tau_{kl} + \rho_{jk}\delta_{il} + \rho_{il}\delta_{kj}). \quad (5)$$

Generally, for phase space variables X_α of operators $\hat{X}_\alpha$, which obey some algebra

$$[\hat{X}_\alpha, \hat{X}_\beta] = i f_{\alpha\beta\gamma}\hat{X}_\gamma \quad (6)$$

with structure constants $f_{\alpha\beta\gamma}$, the classical equations of motion are determined by

$$\frac{dX_\alpha}{dt} = f_{\alpha\beta\gamma}\frac{\partial(\hat{H})_W}{\partial X_\beta} X_\gamma, \quad (7)$$

where $(\hat{H})_W \equiv \mathcal{H}$ is the Weyl symbol of the Hamiltonian [39].

For the phase space variables of the fermionic bilinears and the Hamiltonian of the SYK model this yields

$$i\frac{d}{dt}\rho_{\alpha\beta} = \left(-\frac{\partial\mathcal{H}}{\partial\rho_{\gamma\alpha}}\rho_{\gamma\beta} + \frac{\partial\mathcal{H}}{\partial\tau_{\gamma\alpha}}\tau_{\beta\gamma} - \frac{\partial\mathcal{H}}{\partial\tau_{\alpha\gamma}}\tau_{\beta\gamma}\right) - (\alpha\leftrightarrow\beta)^*$$

$$= \frac{2}{N^{3/2}}\sum_{ijkl}J_{ijkl}\delta_{\alpha l}(\tau_{ji}^*\tau_{\beta k} + \delta_{ik}\rho_{j\beta}) - (\alpha\leftrightarrow\beta)^*,$$

$$i\frac{d}{dt}\tau_{\alpha\beta} = \left(\frac{\partial\mathcal{H}}{\partial\rho_{\alpha\gamma}}\tau_{\gamma\beta} + \frac{\partial\mathcal{H}}{\partial\tau_{\gamma\alpha}^*}\rho_{\gamma\beta} - \frac{\partial\mathcal{H}}{\partial\tau_{\alpha\gamma}^*}\tau_{\gamma\beta}\right) - (\alpha\leftrightarrow\beta)$$

$$= \frac{2}{N^{3/2}}\sum_{ijkl}J_{ijkl}\delta_{\alpha j}(\delta_{il}\tau_{k\beta} - \tau_{kl}\rho_{i\beta}) - (\alpha\leftrightarrow\beta). \quad (8)$$

In the following we will consider uncorrelated initial states that are fully characterized by orbital occupation numbers $n_\alpha = \langle\hat{c}_\alpha^\dagger\hat{c}_\alpha\rangle$. In that case the Wigner function is well approximated by a multivariate Gaussian fixed by the first and second moments [40]. We will be interested in the expansion dynamics starting from an initially imbalanced occupation similar to the situations studied in different recent cold-atom experiments [46–48]. Given this initial state, a suitable observable to consider in the view of echo dynamics is the occupation imbalance

$$\hat{M} = \frac{1}{N}\sum_{\alpha=1}^{N}(2n_\alpha^0 - 1)(2\hat{c}_\alpha^\dagger\hat{c}_\alpha - 1), \quad (9)$$

with Weyl symbol $\mathcal{M} = \frac{2}{N}\sum_{\alpha=1}^{N}(2n_\alpha^0 - 1)\rho_{\alpha\alpha}$, where n_α^0 is the initial value of n_α.

C. Accuracy of the TWA

In order to assess the accuracy of the TWA we compare the result for expansion dynamics from an uncorrelated initial state, where one quarter of the modes is occupied and the rest is empty, with exact dynamics. Figure 1 displays the corresponding time evolution of the occupation imbalance $M(t)$ and the individual mode occupations $n_i(t) = \langle\psi(t)|\hat{c}_i^\dagger\hat{c}_i|\psi(t)\rangle$ for $N = 20$ and a disorder average involving 20 realizations. The dynamics computed using TWA is in good agreement with the exact dynamics. We find empirically that the accuracy of TWA improves as N is increased. As demonstrated in the inset of Fig. 1, the deviations from the exact result are
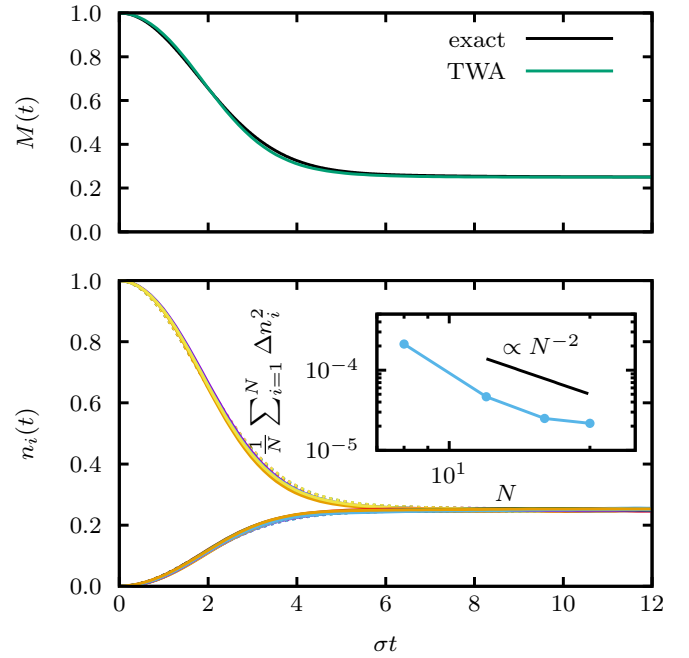

FIG. 1. Comparison of TWA results to the exact dynamics. The top panel shows the time evolution of the occupation imbalance with $N = 20$ modes, whereas in the bottom panel the individual mode occupation numbers are shown. In the bottom panel dashed lines correspond to the exact result. The inset shows the system size dependence of the time-averaged squared deviation of the TWA from the exact result.

compatible with a power law scaling; N^{-2} is shown for orientation.

V. SEMICLASSICAL ECHO DYNAMICS

For our purposes we choose the perturbation Hamiltonian $\hat{H}_p = \sum_\alpha J_\alpha(\hat{c}_\alpha^\dagger\hat{c}_{\alpha+1} + \text{H.c.})$ with normally distributed random couplings J_α (variance $J^2 = \overline{J_\alpha^2}$) and corresponding Weyl symbol $\mathcal{H}_p = 2\sum_\alpha J_\alpha\rho_{\alpha,\alpha+1}$. Note that the dynamics under this Hamiltonian is captured exactly by the TWA because it is quadratic.

A. Echoes in finite systems

In Fig. 2 we compare the result for $\Delta E_M(\tau)$ given in Eq. (3) obtained from TWA with the exact dynamics. The presented data include a disorder average over 80 realizations of both the SYK and the perturbation Hamiltonians. In the initial uncorrelated state one quarter of the sites are filled, and the rest are empty. We find with both methods that the echo deviates increasingly from the initial value as the waiting time τ is increased, and the results are in good agreement at short times. At long times, however, there is a clear discrepancy. In the result obtained from TWA the echo signal ultimately vanishes completely, meaning that $\Delta M(\tau \to \infty) = 3/4$. By contrast, the exact result saturates much earlier. The reason for this is that for finite N the overlap $\langle\psi(\tau)|\hat{P}_{\delta t}|\psi(\tau)\rangle$ is nonzero, resulting in an ever-persisting revival at the echo time [32]. The corresponding saturation value can be determined
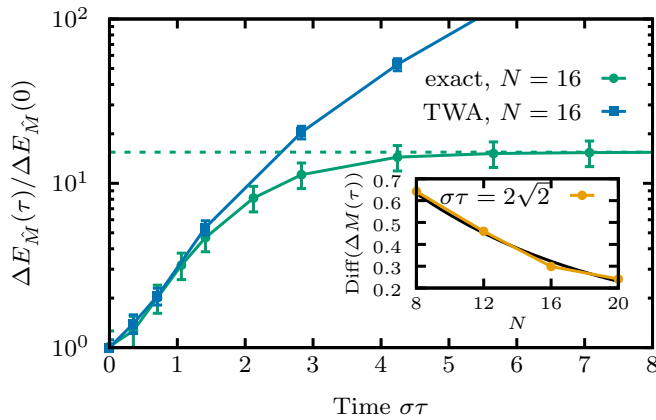
FIG. 2. Echo dynamics computed with TWA in comparison with exact results for $J\delta t = 0.1$ and $N = 16$ at quarter filling. The dashed line indicates the corresponding persistent echo peak height derived in Appendix A. The inset demonstrates that the normalized difference at the echo time is reduced as the system size is increased; the black line corresponds to an exponential fit.

FIG. 3. TWA results for the divergence from the perfect echo computed for $N = 20$ modes. As the perturbation strength δt is decreased, the regime of exponential growth is extended, allowing for the identification of a Lyapunov exponent. The inset shows exact results for system sizes $N = 8, 12, 16, 20$ for $J\delta t = 0.1$. These exact data are compatible with convergence towards the TWA result as $N \to \infty$.

in the exact simulation, and it is indicated in Fig. 2 by the dashed line (see Appendix A for details). This persisting echo, however, vanishes for $N \to \infty$ because, typically, the Loschmidt echo is exponentially suppressed by the system size, $|\langle\psi(\tau)|\hat{P}_{\delta t}|\psi(\tau)\rangle|^2 \sim e^{-Nr(\delta t)}$ with an intensive rate function $r(t)$. Hence, the limits $N \to \infty$ and $\delta t \to 0$ do not commute. Correspondingly, the normalized difference between exact and TWA data at the echo time, Diff$[\Delta E_{\hat{M}}(\tau)]$, is reduced when the system size is increased, as indicated in the inset of Fig. 2. In Appendix A we include further data supporting the anticipated vanishing of the persistent echo in the exact dynamics for $N \to \infty$. This disappearing of an intrinsic difference between TWA and exact echo dynamics goes along with the generally improved accuracy of the TWA as discussed above. Therefore, we expect that in the limit $N \to \infty$ results from TWA and exact dynamics will converge. Since we find in addition that the TWA result for the echo dynamics is independent of N (see Appendix A), we conclude that the TWA results obtained for large but finite N constitute a good approximation of the behavior in the large-N limit.

With our resources for the exact dynamics, however, $N = 20$ is the largest value we can reach due to the large number of nonvanishing matrix elements in the SYK Hamiltonian and the disorder average necessary to perform a meaningful finite-size analysis. For these finite systems the persisting echo can be considered to be a genuine quantum characteristic. The TWA, applicable in the semiclassical limit, does not capture this feature because its origin is the nonvanishing overlap between the quantum states before and after application of the perturbation operator in combination with the unitarity of quantum time evolution.

B. Signature of a butterfly effect in echo dynamics

In Fig. 3 we show TWA results for the divergence from the perfect echo as defined in Eq. (3). After the short time period the data exhibit a clear exponential growth of the difference to the perfect echo, although the observable is bounded. We
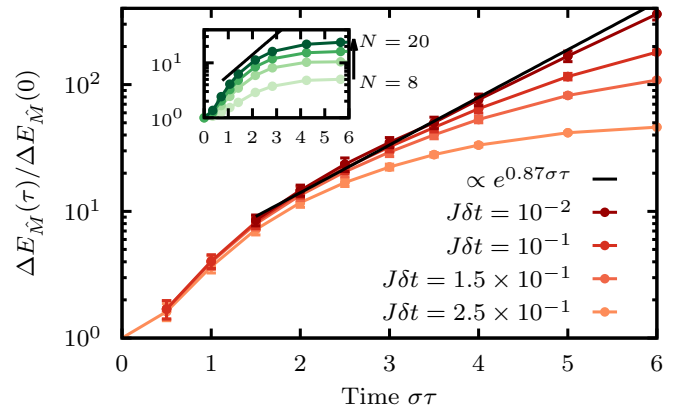
find that the parameter δt, which determines the smallness of the perturbation, controls the extent of the regime, where the exponential law is observed. In direct analogy to classical chaos the exponential divergence of the perturbed echo from the perfect echo allows us to identify a Lyapunov exponent λ_L. A fit to the data in Fig. 3 yields $\lambda_L \approx 0.87\sigma$, which is in good quantitative agreement with a result for the Lyapunov exponent in the limit of high temperature obtained via a diagrammatic large-N expansion and exact numerics [49,50]. Note that our convention for the coupling constants differs from Ref. [50] by a factor of $\sqrt{2}$. In Appendix B we include results for another observable, namely, density-density correlations, showing exponential divergence with the same rate. In the following we will discuss the origin of this exponential divergence in more detail.

C. Role of the double commutator

In the exact echo dynamics we observe that the quadratic term of Eq. (3), in fact, is the only relevant contribution for a large range of perturbation strengths, irrespective of the waiting time. Figure 4(a) shows exact data for $\Delta E_{\hat{M}}(\tau)$ in comparison with the quadratic term $\frac{1}{2}\langle\psi_0|[\hat{H}_p(\tau), [\hat{H}_p(\tau), \hat{M}]]|\psi_0\rangle \delta t^2$ as a function of the perturbation strength δt for different waiting times τ. Both coincide perfectly for $J\delta t < 0.5$.

Even though the TWA does not capture the persistent echo, Fig. 4(b) demonstrates that the semiclassical echo dynamics exhibits the same quadratic dependence on the perturbation strength δt in the regime of exponential growth. Deviations from the quadratic scaling occur only when $\Delta E_{\hat{M}}(\tau)$ begins to saturate. This supports the assertion that in Eq. (3) the second-order term is the single contribution responsible for the exponential sensitivity to the imperfection in the time-reversal protocol.

Similar to the OTOC (1), which is related to the square of the commutator of both operators, $|[V, W(t)]|^2$, expanding the
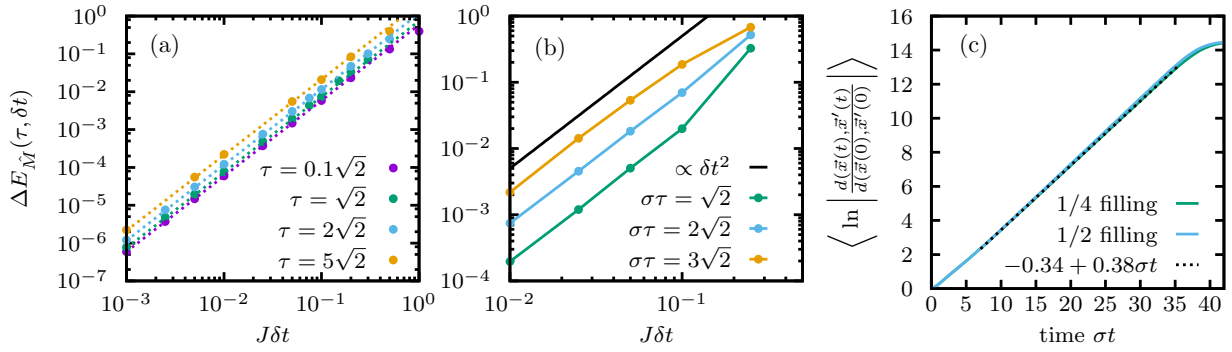
FIG. 4. (a) Echo divergence $\Delta M(\tau)$ for different fixed τ as a function of the perturbation strength δt. Comparison of data obtained from exact full echo dynamics (dots) with the quadratic term in Eq. (3) alone (dashed lines). The double commutator is the single contribution to the echo divergence over a large range of τ and δt. (b) Corresponding TWA result. (c) Average divergence of initially close-by trajectories in phase space under TWA dynamics. A linear fit yields the estimate for the classical Lyapunov exponent.

double commutator reveals an out-of-time-order structure:

$$[\hat{H}_p(\tau), [\hat{H}_p(\tau), \hat{M}]]$$
$$= \hat{H}_p(\tau)^2 \hat{M} + \hat{M}\hat{H}_p(\tau)^2 - 2\hat{H}_p(\tau)\hat{M}\hat{H}_p(\tau). \quad (10)$$

In this expression the last term accounts for the butterfly effect. For an extensive perturbation Hamiltonian $\hat{H}_p$ the double commutator becomes extensive at late times. In the thermodynamic limit the double commutator can grow indefinitely, such that it can govern the exponential divergence from the perfect echo irrespective of the higher-order terms as long as $\langle\psi_0|[\hat{H}_p(\tau), [\hat{H}_p(\tau), \hat{M}]]|\psi_0\rangle \delta t^2 \ll 1$. We deduce that only at late times do higher-order terms become important, resulting in the approach to a constant.

The inference that the double commutator governs the exponential divergence in the echo dynamics is supported by the relation to the Lyapunov exponent of the classical TWA equations, which is discussed next.

D. Classical Lyapunov exponent of the TWA equations

The Lyapunov exponent occurring in the semiclassical echo dynamics can be related to the largest Lyapunov exponent of the dynamical system defined by the TWA equations of motion. The largest classical Lyapunov exponent is defined as

$$\lambda_{\text{cl}} = \left\langle \lim_{t\to\infty} \lim_{d(\vec{x}(0),\vec{x}'(0))\to 0} \frac{1}{t} \ln\left|\frac{d(\vec{x}(t),\vec{x}'(t))}{d(\vec{x}(0),\vec{x}'(0))}\right| \right\rangle, \quad (11)$$

with coordinate vectors $\vec{x}(t)$ and $\vec{x}'(t)$ and $d(\vec{x},\vec{x}') = \sqrt{\sum_i (x_i - x_i')^2}$ being the Euclidian distance. The time dependence of the coordinate vectors is given by the equations of motion, and $\langle\cdot\rangle$ indicates the classical average over an ensemble of trajectories.

To estimate the Lyapunov exponent of the TWA equations of motion we average the divergence of an ensemble of initially close-by trajectories on a fixed time interval; details are given in Appendix C. Figure 4(c) displays the resulting average $\langle\ln|d(\vec{x}(t),\vec{x}'(t))/d(\vec{x}(0),\vec{x}'(0))|\rangle$, which we computed for half and quarter fillings with $d_0 = 10^{-8}$. We find a clear linear dependence on time, and a fit yields the classical Lyapunov exponent $\lambda_{\text{cl}} \approx 0.34$. The result varies only weakly as the filling is changed.

This value of λ_{cl} is slightly less than half of λ_L, which we extracted before from the echo dynamics. In the following we will argue that a factor of 2 between both is to be expected. We attribute the slight discrepancy to the different orders of averaging and taking the logarithm, resulting in a slightly smaller classical Lyapunov exponent, as reported in Ref. [34].

The Weyl symbol of the double commutator in Eq. (10) can be written in the form

$$([\hat{H}_p(\tau), [\hat{H}_p(\tau), \hat{M}]])_W$$
$$= A_j^i \frac{\partial x_i(t)}{\partial x_j(0)} + B_j^i \frac{\partial x_i(0)}{\partial x_j(t)} + C_{ij}^{kl} \frac{\partial x_k(t)}{\partial x_i(0)} \frac{\partial x_l(0)}{\partial x_j(t)}, \quad (12)$$

with $\vec{x}$ being the vector of ρ and τ coordinates of the TWA equations (see Appendix D). The modulus of all derivatives occurring in this expression grows with the classical Lyapunov exponent. However, the sums of the single derivatives in the first two terms will cancel because they correspond to the linear response. Hence, if the terms in the quadratic contribution do not cancel, at late times

$$([\hat{H}_p(\tau), [\hat{H}_p(\tau), \hat{M}]])_W \sim e^{2\lambda_{\text{cl}}t}. \quad (13)$$

The Weyl symbols of higher-order commutators would contain growth rates that are higher multiples of λ_{cl}. Since we only observe the factor of 2 in the echo dynamics, we conclude that the quadratic term in Eq. (3) is, in fact, the one that is relevant for the butterfly effect.

VI. ON THE IMPORTANCE OF INCLUDING QUANTUM FLUCTUATIONS

It is worthwhile to elaborate more on the importance of quantum fluctuations for the dynamics of the SYK model in the semiclassical limit. In the following we will contrast mean-field dynamics, which captures only fluctuations on the Gaussian level of single-fermion operators, against dynamics, which includes fluctuations that are Gaussian on the level of fermionic bilinears.

The TWA equations of motion presented in Sec. IV B are essentially mean-field equations of motion. In the following we aim to outline the key difference between TWA and the mean-field approximation, namely, the fact that TWA captures

fluctuations which are essential for the dynamics of the SYK model. The importance of fluctuations is due to the fact that the microscopic degrees of freedom are fermions, which are always strongly fluctuating. This is, for example, in contrast to the semiclassical limit of large spins, where the fluctuations vanish in the limit of large spin.

The most general equations of motion for a mean-field approximation are

$$i\frac{d}{dt}\rho_{\alpha\beta} = \frac{2}{N^{3/2}}\sum_{ijkl}J_{ijkl}\delta_{\alpha l}(\tau_{ji}^*\tau_{\beta k} + \delta_{ik}\rho_{j\beta} + 2\rho_{j\beta}\rho_{ik})$$
$$- (\alpha \leftrightarrow \beta)^*,$$

$$i\frac{d}{dt}\tau_{\alpha\beta} = \frac{2}{N^{3/2}}\sum_{ijkl}J_{ijkl}\delta_{j\alpha}(\delta_{il}\tau_{k\beta} - \rho_{i\beta}\tau_{kl} - 2\rho_{il}\tau_{\beta k})$$
$$- (\alpha \leftrightarrow \beta). \quad (14)$$

These equations are obtained under the assumption that the quantum state remains Gaussian at all times. In that case the Wick theorem can be used to split all higher-order correlations into products of two-point functions, which correspond to the resulting phase space variables.

The mean-field Hamiltonian corresponding to Eq. (14) incorporates all possibilities, meaning that there are classical fields coupling to pairing terms as well as hopping and local potentials. It turns out (see Fig. 6 below) that to approximate the SYK dynamics it is sufficient to consider a much simpler mean-field Hamiltonian including only pairing operators, given that the quantum fluctuations in the initial state are taken into account. This simpler mean-field Hamiltonian takes the form

$$\hat{H} = \frac{1}{\sqrt{2N}}\sum_{ij}[\Delta_{ij}(t)\hat{c}_i^\dagger\hat{c}_j^\dagger + \text{H.c.}], \quad (15)$$

where the classical field

$$\Delta_{ij}(t) = \frac{1}{2N}\sum_{kl}J_{ijkl}\langle\hat{c}_k\hat{c}_l\rangle_t = \frac{1}{2N}\sum_{kl}J_{ijkl}\tau_{kl}(t) \quad (16)$$

is determined self-consistently. The resulting equations of motion constitute a reduction of Eq. (8):

$$i\frac{d\rho_{\alpha\beta}}{dt} = -\frac{2}{\sqrt{2N}}\sum_k\Delta_{k\alpha}(t)^*\tau_{\beta k} - (\alpha \leftrightarrow \beta)^*,$$

$$i\frac{d\tau_{\alpha\beta}}{dt} = \frac{2}{\sqrt{2N}}\sum_j\Delta_{\alpha j}(t)\rho_{j\beta} - (\alpha \leftrightarrow \beta). \quad (17)$$

In the mean-field approximation the initial condition of the phase space variables is fixed by the expectation values in the initial state,

$$\rho_{\alpha\beta}(0) = \langle\hat{c}_\alpha^\dagger\hat{c}_\beta\rangle_{t=0} - \frac{\delta_{\alpha\beta}}{2},$$

$$\tau_{\alpha\beta}(0) = \langle\hat{c}_\alpha\hat{c}_\beta\rangle_{t=0} = 0. \quad (18)$$

This means, however, that mean-field dynamics with Eq. (17) is trivial because $\langle\hat{c}_i\hat{c}_j\rangle_{t=0} = 0$; in the mean-field approximation the system remains stationary at all times. Nontrivial dynamics is initiated only by fluctuations of the fermionic bilinears in the initial state. These fluctuations can be included
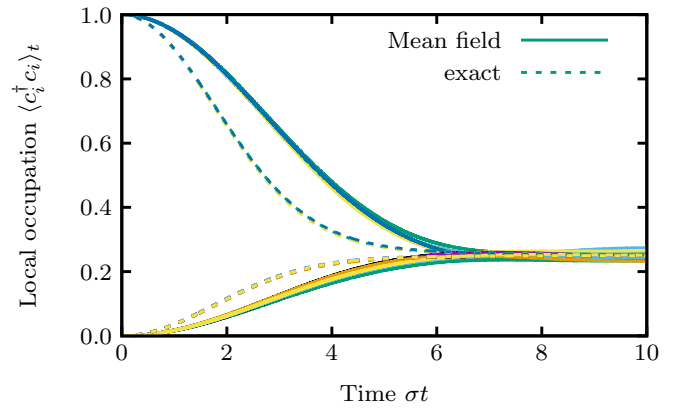

FIG. 5. Expansion dynamics from the uncorrelated initial state as observed in the single-mode occupation numbers $n_i(t) = \langle\hat{c}_i^\dagger\hat{c}_i\rangle_t$. The solid lines correspond to mean-field dynamics based on the most general equations of motion, Eq. (14). The dashed lines were obtained by computing the full quantum dynamics. The data shown are for $N = 20$ at quarter filling.

by stochastic sampling of the initial condition, as we will discuss below.

Within the mean-field approximation nontrivial dynamics is obtained when considering the equations of motion given in Eq. (14). These equations account for Gaussian fluctuations on the level of single-fermion operators. Figure 5 shows the result for relaxation dynamics obtained in the mean-field approximation using Eq. (14) starting with an uncorrelated state with an occupation imbalance. Although the general shape of the decay is captured quite well, the decay timescale differs from the corresponding exact result. In the mean-field approximation the relaxation turns out to be too slow. This discrepancy between mean-field dynamics and exact dynamics was already observed in Ref. [39], where, however, different mean-field approximations were considered.

In order to accurately describe the relaxation dynamics it is essential to capture fluctuations of the fermionic bilinears correctly. This can be achieved by including Gaussian fluctuations of the phase space variables [51] by stochastic sampling and an averaging of the resulting trajectories. This approach is essentially equivalent to stochastic sampling from the Wigner function of the initial state, as it is done in the TWA. Figure 6 displays the result for relaxation dynamics obtained in this approximation using the equations of motion of the simple mean-field Hamiltonian, Eq. (17), supplemented with fluctuations of the initial conditions. The comparison with the exact result shows very good agreement. Hence, we conclude that the relaxation dynamics is mainly driven by two-particle fluctuations, which are included in the TWA but not in the mean-field approximation.

A similar approach to incorporate quantum fluctuations in phase space dynamics was already introduced in Ref. [52]. However, as is evident from the discussion above, there are various ambiguities for which there is no *a priori* resolution. Nevertheless, the corresponding choices might affect the resulting physical quantities. For example, the additional terms occurring in Eq. (14), which are irrelevant for the dynamics in our case, might be important under different
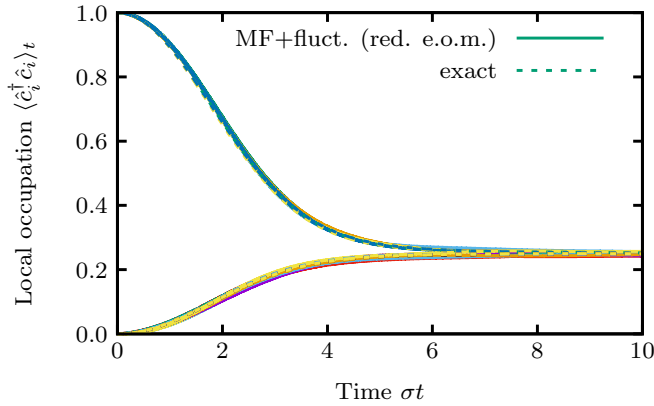
FIG. 6. Expansion dynamics from the uncorrelated initial state as observed in the single-mode occupation numbers $n_i(t) = \langle \hat{c}_i^\dagger \hat{c}_i \rangle_t$. The solid lines correspond to dynamics obtained based on the reduced mean-field equations of motion, Eq. (17), including fluctuations in the initial state by stochastic sampling of the initial conditions. The dashed lines were obtained by computing the full quantum dynamics. The data shown are for $N = 20$ at quarter filling.

circumstances [41]. The TWA provides a consistent mathematical framework to set up the equations of motion and to incorporate fluctuations. The remaining ambiguity in choosing the bilinears based on which the phase space is constructed corresponds to finding the decoupling scheme where the saddle point approximation becomes asymptotically exact (see Sec. IV A).

As a final remark we would like to mention that the short-comings of the mean-field approximation are also reflected in the fact that with the mean field only a subextensive part of the spectrum can be captured [35] and only fluctuations as included in TWA render the energies extensive.

VII. DISCUSSION

We found that the exponential divergence from the perfect echo in the semiclassical dynamics is due to the growth of an out-of-time-order double commutator of the form $[\hat{V}(\tau), [\hat{V}(\tau), \hat{W}(0)]]$. This assertion is based on the small perturbation expansion in Eq. (3), which does not rely on any semiclassical approximation. In future work the structure and characteristic behavior of these objects should be further explored, in particular with regard to the sensitivity of genuine quantum dynamics far from a classical limit to small perturbations.

Regarding irreversibility our result implies that the dynamics of the SYK model is irreversible in the same sense as a chaotic classical system: Any imperfection in the time-reversal procedure leads to an exponential divergence from the perfect echo, and substantial improvement is prohibitively expensive because the Lyapunov exponent is perturbation independent.

APPENDIX A: FINITE-SIZE ANALYSIS

For finite mode number N the perturbed state will always have a nonvanishing overlap with the unperturbed state, $|\langle \psi(\tau)|\hat{P}_{\delta t}|\psi(\tau)\rangle| > 0$. Accordingly, we can decompose $\hat{P}_{\delta t}|\psi(\tau)\rangle = \cos(\alpha_{\delta t})|\psi(\tau)\rangle + \sin(\alpha_{\delta t})|\phi\rangle$ by introducing the "orthogonal component" $|\phi\rangle$, with $\langle \psi(\tau)|\phi\rangle = 0$. Considering this decomposition, it becomes evident that the remaining "parallel component" of the perturbed state leads to an ever-persisting echo at time $t = 2\tau$:

$$\langle \psi(\tau)|\hat{P}_{\delta t}^\dagger e^{-i\hat{H}\tau}\hat{M}e^{i\hat{H}\tau}\hat{P}_{\delta t}|\psi(\tau)\rangle$$

$$= \cos^2(\alpha_{\delta t})\langle \psi_0|\hat{M}|\psi_0\rangle + \sin^2(\alpha_{\delta t})\langle \phi|e^{-i\hat{H}\tau}\hat{M}e^{i\hat{H}\tau}|\phi\rangle$$

$$+ \sin(2\alpha_{\delta t})\text{Re}(\langle \psi_0|\hat{M}e^{i\hat{H}\tau}|\phi\rangle). \quad (A1)$$

For finite N there is a time-independent contribution proportional to the initial value of the observable, $\langle \psi_0|\hat{M}|\psi_0\rangle$, and the overlap of the perturbed and unperturbed states, $\cos^2(\alpha_{\delta t}) = |\langle \psi(\tau)|\hat{P}_{\delta t}|\psi(\tau)\rangle|^2$. At late times the expectation value in the second term will attain an equilibrium value $M_\phi^\infty = \lim_{\tau\to\infty}\langle \phi|e^{-i\hat{H}\tau}\hat{M}e^{i\hat{H}\tau}|\phi\rangle$, and the overlap in the third term will vanish. Therefore, the persistent-echo peak height at large τ is given by

$$\lim_{\tau\to\infty} E_{\hat{M}}(\tau) = \cos^2(\alpha_{\delta t})\langle \psi_0|\hat{M}|\psi_0\rangle + \sin^2(\alpha_{\delta t})M_\phi^\infty. \quad (A2)$$

Exemplary results for the dynamics including effective time reversal are shown in Fig. 7. In the thermodynamic limit, $N \to \infty$, we will have $\alpha_{\delta t} = \pi/2$; that is, the contribution given by the initial expectation value of $\hat{M}$ vanishes, and we obtain

$$\lim_{N\to\infty}\lim_{\tau\to\infty} E_{\hat{M}}(\tau) = M_\phi^\infty. \quad (A3)$$

Moreover, the window for possible exponential divergence from the perfect echo has a fixed size for a given finite N. This window cannot be increased by reducing δt, which is evident from Eq. (3) of the main text. In a finite system the expectation value of the double commutator is bounded for all times τ, $|\langle \psi_0|[\hat{H}_p(\tau), [\hat{H}_p(\tau), \hat{O}]]|\psi_0\rangle| < C(N)$. Therefore, in the limit of small δt

$$1 \leqslant \left|\frac{\Delta E_{\hat{O}}(\tau)}{\Delta E_{\hat{O}}(0)}\right| < \frac{C(N)}{|\langle \psi_0|[\hat{H}_p, [\hat{H}_p, \hat{O}]]|\psi_0\rangle|}. \quad (A4)$$

In the following we present data for the variation of the echo signal $E_{\hat{M}}(\tau)$ with changing system sizes, which supports our assertion that the persistent echo vanishes in exact quantum dynamics. For a faithful investigation of finite-size effects disorder averaging is essential because fluctuations introduced by adding new randomly coupled degrees of freedom can otherwise spoil the analysis.
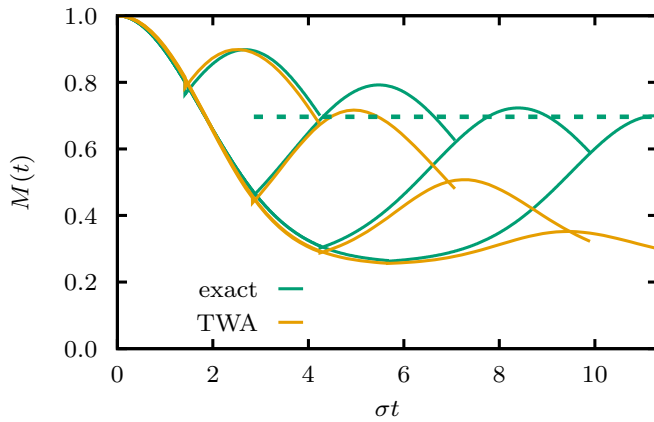
FIG. 7. Full time evolution under imperfect effective time reversal as obtained by TWA in comparison with exact dynamics for different forward times τ with system size $N = 20$ at quarter filling and $J\delta t = 0.25$. The exact dynamics show a persistent echo signal, whereas the TWA echo vanishes at long forward times. The dashed line indicates the persistent peak height as given by Eq. (A2).

In Fig. 8 we show exact results for the divergence from the perfect echo for different system sizes, including a disorder average over 80 realizations. The dashed lines indicate the saturation value of the persistent echo computed directly according to Eq. (A2), where at quarter filling $M_\phi^\infty = 1/4$. We find very good agreement of the echo at late times with this value. As discussed in the main text and earlier in this section the saturation value increases as the system size is increased. This corresponds to the vanishing of the persistent echo in the thermodynamic limit.

Figure 9 displays TWA results for the divergence from the perfect echo for different system sizes. In this case we find that the results are almost identical despite a doubling of the system size.

Combining both results with the expectation that TWA becomes exact in the thermodynamic limit we conclude that the TWA result gives already at finite system sizes a good approximation of the result in the thermodynamic limit and with increasing N the exact results will converge to this.
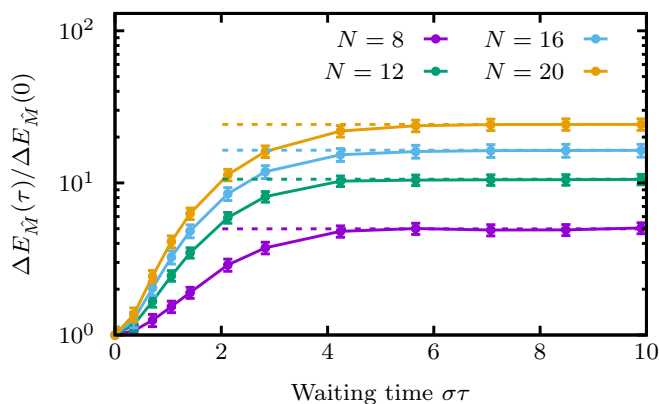

FIG. 8. Finite-size analysis of exact results for the echo dynamics. The dashed lines indicate the saturation values obtained from the overlap of the perturbed with the unperturbed state. Here, $J\delta t = 0.1$.
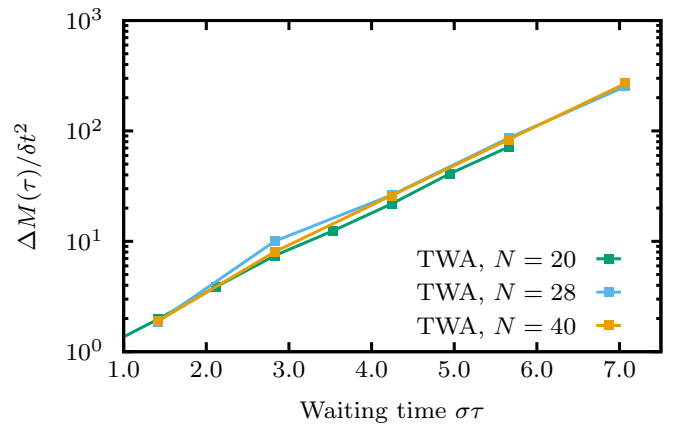

FIG. 9. Finite-size analysis of results for the echo dynamics obtained using TWA.

APPENDIX B: ECHO IN DENSITY-DENSITY CORRELATION

In addition to the occupation imbalance $\hat{M}$ presented in the main text we investigated echoes in density-density correlations. We consider the average correlation

$$\mathcal{C}(t) = \frac{2}{N(N-1)} \sum_{i<j} |\langle \hat{n}_i \hat{n}_j \rangle_t - \langle \hat{n}_i \rangle_t \langle \hat{n}_j \rangle_t|, \qquad \text{(B1)}$$

with $\hat{n}_i = \hat{c}_i^\dagger \hat{c}_i$.

Figure 10 shows the dynamics of the echo $E_\mathcal{C}(\tau)$ as defined in Eq. (2). With increasing waiting time τ we find also for the correlation average $\mathcal{C}$ an exponential divergence from the perfect echo. The exponential rate is the same as in the case of the occupation imbalance.
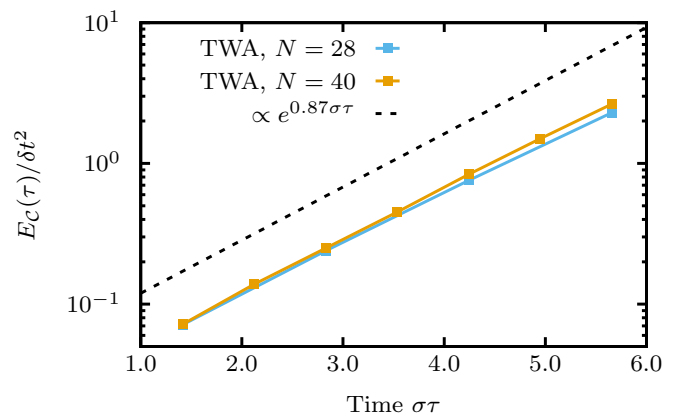

FIG. 10. Echo observed in the correlation average $\mathcal{C}$ [see Eq. (B1)] as a function of waiting time τ. The exponential rate is the same as in the case of the occupation imbalance.

APPENDIX C: APPROACH TO DETERMINE THE CLASSICAL LYAPUNOV EXPONENT

A common numerical method to determine the largest classical Lyapunov exponent

$$\lambda_{\rm cl} = \left\langle \lim_{t\to\infty} \lim_{d(\vec{x}(0),\vec{x}'(0))\to 0} \frac{1}{t} \ln \left| \frac{d(\vec{x}(t),\vec{x}'(t))}{d(\vec{x}(0),\vec{x}'(0))} \right| \right\rangle \qquad (C1)$$

is to integrate the equations of motion of two close-by initial conditions $\vec{x}(0)$ and $\vec{x}'(0)$ with a small fixed $d(\vec{x}(0),\vec{x}'(0)) = d_0$ and evaluate the ratio $d(\vec{x}(t),\vec{x}'(t))/d_0$ at a fixed time t. Then $\vec{x}'$ is reinitialized such that $d(\vec{x}(t),\vec{x}'(t)) = d_0$ and the equations of motion are integrated for another interval t before the ratio of initial and final distances is evaluated again. This procedure is iterated, and the samples of $t^{-1} \ln |d(\vec{x}(t),\vec{x}'(t))/d(\vec{x}(0),\vec{x}'(0))|$ are averaged to obtain an estimate of the classical Lyapunov exponent (C1).

To estimate the Lyapunov exponent of the TWA equations of motion we employed a similar approach. In this case $\vec{x} \equiv (\rho_{\alpha,\beta}, \tau_{\alpha,\beta})$. During a sequence of integration and reinitializa-

tion in turns we average $\ln |d(\vec{x}(t),\vec{x}'(t))/d(\vec{x}(0),\vec{x}'(0))|$ on the whole interval $0 < t < t_{\max}$. Additionally, we average over many such sequences with initial conditions drawn from the Wigner function of the initial state under consideration. In this way we obtained the result shown in Fig. 4(c) in the main text.

APPENDIX D: STRUCTURE OF THE WEYL SYMBOL OF THE DOUBLE COMMUTATOR

Let us denote the set of phase space variables by $\vec{x}$. In our case both H_p and M are linear in TWA variables, which means that the Bopp operators take the forms

$$\vec{H}_p = h(\vec{x}) + \sum_i h_i(\vec{x}) \frac{\partial}{\partial x_i} \qquad (D1)$$

and

$$\vec{M} = m(\vec{x}) + \sum_i m_i(\vec{x}) \frac{\partial}{\partial x_i}, \qquad (D2)$$

where $h(\vec{x})$, $h_i(\vec{x})$, $m(\vec{x})$, and $m_i(\vec{x})$ are some functions of the coordinates.

Plugging this into the double commutator yields the Weyl symbol

$$
\begin{aligned}
([\hat{H}_p(t), [\hat{H}_p(t), \hat{M}]])_W &= \left[h(\vec{x}(t)) + \sum_i h_i(\vec{x}(t)) \frac{\partial}{\partial x_i(t)} \right] \left[h(\vec{x}(t)) + \sum_j h_j(\vec{x}(t)) \frac{\partial}{\partial x_j(t)} \right] m(\vec{x}) \\
&+ \left[m(\vec{x}) + \sum_i m_i(\vec{x}) \frac{\partial}{\partial x_i} \right] \left[h(\vec{x}(t)) + \sum_j h_j(\vec{x}(t)) \frac{\partial}{\partial x_j(t)} \right] h(\vec{x}(t)) \\
&- 2 \left[h(\vec{x}(t)) + \sum_i h_i(\vec{x}(t)) \frac{\partial}{\partial x_i(t)} \right] \left[m(\vec{x}) + \sum_j m_j(\vec{x}) \frac{\partial}{\partial x_j} \right] h(\vec{x}(t)) \\
&= \sum_{ij} h_i(\vec{x}(t)) h_j(\vec{x}(t)) \frac{\partial}{\partial x_i(t)} \frac{\partial}{\partial x_j(t)} m(\vec{x}) + \sum_{ij} h_i(\vec{x}(t)) \frac{\partial h_j(\vec{x}(t))}{\partial x_i(t)} \frac{\partial}{\partial x_j(t)} m(\vec{x}) \\
&- 2 \sum_{ij} h_i(\vec{x}(t)) \frac{\partial m_j(\vec{x})}{\partial x_i(t)} \frac{\partial h(\vec{x}(t))}{\partial x_j} + \sum_{ij} m_i(\vec{x}) \frac{\partial h(\vec{x}(t))}{\partial x_j(t)} \frac{\partial}{\partial x_i} h_j(\vec{x}(t)) \\
&- \sum_{ij} m_i(\vec{x}) h_j(\vec{x}(t)) \frac{\partial}{\partial x_i} \frac{\partial h(\vec{x}(t))}{\partial x_j(t)}.
\end{aligned} \qquad (D3)
$$

Now we use the chain rule $\frac{\partial f(x_i(t_1))}{\partial x_j(t_2)} = \sum_k \frac{f(x_i(t_1))}{\partial x_k(t_1)} \frac{\partial x_k(t_1)}{\partial x_j(t_2)}$ wherever applicable, yielding

$$
\begin{aligned}
&([\hat{H}_p(t), [\hat{H}_p(t), \hat{M}]])_W \\
&= \sum_{ijkl} \left[h_i(\vec{x}(t)) h_j(\vec{x}(t)) \frac{\partial^2 m(\vec{x})}{\partial x_k \partial x_l} \right] \frac{\partial x_k}{\partial x_i(t)} \frac{\partial x_l}{\partial x_j(t)} + \sum_{jk} \left[\sum_i h_i(\vec{x}(t)) \frac{\partial h_j(\vec{x}(t))}{\partial x_i(t)} \frac{\partial m(\vec{x})}{\partial x_k} \right] \frac{\partial x_k}{\partial x_j(t)} \\
&- 2 \sum_{ijkl} \left[h_i(\vec{x}(t)) \frac{\partial m_j(\vec{x})}{\partial x_k} \frac{\partial h(\vec{x}(t))}{\partial x_l(t)} \right] \frac{\partial x_k}{\partial x_i(t)} \frac{\partial x_l(t)}{\partial x_j} + \sum_{ik} \left[\sum_j m_i(\vec{x}) \frac{\partial h(\vec{x}(t))}{\partial x_j(t)} \frac{\partial h_j(\vec{x}(t))}{\partial x_k(t)} \right] \frac{\partial x_k(t)}{\partial x_i} \\
&- \sum_{ik} \left[\sum_j m_i(\vec{x}) h_j(\vec{x}(t)) \frac{\partial^2 h(\vec{x}(t))}{\partial x_k(t) \partial x_j(t)} \right] \frac{\partial x_k(t)}{\partial x_i}.
\end{aligned} \qquad (D4)
$$

Since in our case $h(\vec{x})$ and $m(\vec{x})$ are linear in $\vec{x}$, the expression can be simplified to

$$([\hat{H}_p(t), [\hat{H}_p(t), \hat{M}]])_W = \sum_{jk} \left[\sum_i h_i(\vec{x}(t)) \frac{\partial h_j}{\partial x_i} \frac{\partial m}{\partial x_k} \right] \frac{\partial x_k}{\partial x_j(t)}$$

$$- 2 \sum_{ijkl} \left[h_i(\vec{x}(t)) \frac{\partial m_j}{\partial x_k} \frac{\partial h}{\partial x_l} \right] \frac{\partial x_k}{\partial x_i(t)} \frac{\partial x_l(t)}{\partial x_j} + \sum_{ik} \left[\sum_j m_i(\vec{x}) \frac{\partial h}{\partial x_j} \frac{\partial h_j}{\partial x_k} \right] \frac{\partial x_k(t)}{\partial x_i}. \tag{D5}$$

In this form the Weyl symbol corresponds to Eq. (12) in the main text. This expression involves linear-response-type terms, which are linear in $\frac{\partial x_i(t)}{\partial x_j(0)}$, and terms that are quadratic in these derivatives. The linear terms should cancel such that they do not contribute to exponential growth; otherwise, the response of the form $\{\hat{H}_p(\tau)^2, \hat{M}\} = \hat{H}_p(\tau)^2 \hat{M} + \hat{M}\hat{H}_p(\tau)^2$ would also grow exponentially.

[1] P. Hayden and J. Preskill, J. High Energy Phys. 09 (2007) 120.

[2] Y. Sekino and L. Susskind, J. High Energy Phys. 10 (2008) 065.

[3] S. H. Shenker and D. Stanford, J. High Energy Phys. 12 (2014) 46.

[4] A. Kitaev (unpublished), http://online.kitp.ucsb.edu/online/joint98/kitaev/.

[5] A. I. Larkin and Y. N. Ovchinnikov, Zh. Eksp. Teor. Fiz. **55**, 2262 (1968) [Sov. Phys. JETP **28**, 1200 (1969)].

[6] J. Maldacena, S. H. Shenker, and D. Stanford, J. High Energy Phys. 08 (2016) 106.

[7] A. Kitaev (unpublished), http://online.kitp.ucsb.edu/online/entangled15/kitaev/; http://online.kitp.ucsb.edu/online/entangled15/kitaev2/.

[8] J. Maldacena and D. Stanford, Phys. Rev. D **94**, 106002 (2016).

[9] S. Sachdev and J. Ye, Phys. Rev. Lett. **70**, 3339 (1993).

[10] S. Sachdev, Phys. Rev. Lett. **105**, 151602 (2010).

[11] A. Bohrdt, C. B. Mendl, M. Endres, and M. Knap, New J. Phys. **19**, 063001 (2017).

[12] Y. Huang, Y.-L. Zhang, and X. Chen, Ann. Phys. (Berlin, Ger.) **529**, 1600318 (2017).

[13] X. Chen, T. Zhou, D. A. Huse, and E. Fradkin, Ann. Phys. (Berlin, Ger.) **529**, 1600332 (2017).

[14] E. Iyoda and T. Sagawa, Phys. Rev. A **97**, 042330 (2018).

[15] B. Swingle and D. Chowdhury, Phys. Rev. B **95**, 060201(R) (2017).

[16] H. Shen, P. Zhang, R. Fan, and H. Zhai, Phys. Rev. B **96**, 054503 (2017).

[17] A. A. Patel, D. Chowdhury, S. Sachdev, and B. Swingle, Phys. Rev. X **7**, 031047 (2017).

[18] R. Fan, P. Zhang, H. Shen, and H. Zhai, Sci. Bull. **62**, 707 (2017).

[19] L. D'Alessio, Y. Kafri, A. Polkovnikov, and M. Rigol, Adv. Phys. **65**, 239 (2016).

[20] C. Gogolin and J. Eisert, Rep. Prog. Phys. **79**, 056001 (2016).

[21] W. Thompson, Proc. R. Soc. Edinburgh **8**, 325 (1874).

[22] L. Boltzmann, Sitzungsber. Akad. Wiss. Wien **66**, 275 (1872).

[23] J. Loschmidt, Sitzungsber. Akad. Wiss. Wien **73**, 128 (1876).

[24] L. Boltzmann, Sitzungsber. Akad. Wiss. Wien **75**, 67 (1877).

[25] A. Peres, Phys. Rev. A **30**, 1610 (1984).

[26] T. Gorin, T. Prosen, T. H. Seligman, and M. Žnidarič, Phys. Rep. **435**, 33 (2006).

[27] P. Jacquod and C. Petitjean, Adv. Phys. **58**, 67 (2009).

[28] B. V. Fine, T. A. Elsayed, C. M. Kropf, and A. S. de Wijn, Phys. Rev. E **89**, 012923 (2014).

[29] T. A. Elsayed and B. V. Fine, Phys. Scr. **2015**, 014011.

[30] P. R. Zangara, D. Bendersky, and H. M. Pastawski, Phys. Rev. A **91**, 042112 (2015).

[31] M. Schmitt and S. Kehrein, Europhys. Lett. **115**, 50001 (2016).

[32] M. Schmitt and S. Kehrein, Phys. Rev. B **98**, 180301(R) (2018).

[33] A. E. Tarkhov, S. Wimberger, and B. V. Fine, Phys. Rev. A **96**, 023624 (2017).

[34] E. B. Rozenbaum, S. Ganeshan, and V. Galitski, Phys. Rev. Lett. **118**, 086801 (2017).

[35] T. Scaffidi and E. Altman, arXiv:1711.04768 .

[36] V. Khemani, D. A. Huse, and A. Nahum, Phys. Rev. B **98**, 144304 (2018).

[37] B. Swingle, Nat. Phys. **14**, 988 (2018).

[38] M. Gärttner, J. G. Bohnet, A. Safavi-Naini, M. L. Wall, J. J. Bollinger, and A. M. Rey, Nat. Phys. **13**, 781 (2017).

[39] S. M. Davidson, D. Sels, and A. Polkovnikov, Ann. Phys. (NY) **384**, 128 (2017).

[40] S. M. Davidson, Ph.D. thesis, Boston University, 2017.

[41] A. Polkovnikov, Ann. Phys. (NY) **325**, 1790 (2010).

[42] A. Altland, V. Gurarie, T. Kriecherbauer, and A. Polkovnikov, Phys. Rev. A **79**, 042703 (2009).

[43] A. Piñeiro Orioli, A. Safavi-Naini, M. L. Wall, and A. M. Rey, Phys. Rev. A **96**, 033607 (2017).

[44] A. Eberlein, V. Kasper, S. Sachdev, and J. Steinberg, Phys. Rev. B **96**, 205123 (2017).

[45] L. G. Yaffe, Rev. Mod. Phys. **54**, 407 (1982).

[46] U. Schneider, L. Hackermüller, J. P. Ronzheimer, S. Will, S. Braun, T. Best, I. Bloch, E. Demler, S. Mandt, D. Rasch, and A. Rosch, Nat. Phys. **8**, 213 (2012).

[47] J.-y. Choi, S. Hild, J. Zeiher, P. Schauß, A. Rubio-Abadal, T. Yefsah, V. Khemani, D. A. Huse, I. Bloch, and C. Gross, Science **352**, 1547 (2016).

[48] P. Bordia, H. Lüschen, S. Scherg, S. Gopalakrishnan, M. Knap, U. Schneider, and I. Bloch, Phys. Rev. X **7**, 041047 (2017).

[49] B. Kobrin, C. Olund, D. Stanford, J. Moore, and N. Yao (unpublished).

[50] D. A. Roberts, D. Stanford, and A. Streicher, J. High Energy Phys. 06 (2018) 122.

[51] Note that Gaussian fluctuations on the level of the phase space variables (fermionic bilinears) include the connected parts of the fermionic four-point function.

[52] K. Damle, S. N. Majumdar, and S. Sachdev, Phys. Rev. A **54**, 5037 (1996).

[53] C. Sanderson and R. Curtin, J. Open Source Software **1**, 26 (2016).

[54] ITENSOR, http://www.itensor.org/.